Atomic Force Microscope Imaging Contrast Based on Molecular Recognition

M. Ludwig, W. Dettmann, and H. E. Gaub
Lehrstuhl für Angewandte Physik, Ludwig Maximilians Universität, 80799 München, Germany

ABSTRACT The contrast in atomic force microscope images arises from forces between the tip and the sample. It was shown recently that specific molecular interaction forces may be measured with the atomic force microscope; consequently, we use such forces to map the distribution of binding partners on samples. Here we demonstrate this concept by imaging a streptavidin pattern with a biotinylated tip in a novel imaging mode called affinity imaging. In this mode topography, adhesion, and sample elasticity are extracted online from local force scans. We show that this technique allows the separation of these values and that the measured binding pattern is based on specific molecular interactions.

INTRODUCTION

The scanning probe microscopes (Binnig et al., 1986; Binnig et al., 1983; Hansma et al., 1988) have evolved into universal instruments for experiments on the nanoscopic length scale (Wickramasinghe, 1990). Particularly in the life sciences, the atomic force microscope (AFM) has been established as the most widely used variant of this family (Engel, 1991; Hansma and Hoh, 1994; Radmacher et al., 1992). A broad spectrum of key experiments has demonstrated its ability to image biological samples under quasi-physiological conditions at length scales ranging from the cellular (Henderson et al., 1992) to the molecular level (Bezanilla et al., 1994; Hoh et al., 1991; Müller et al., 1996; Weisenhorn et al., 1990). Moreover, dynamic processes have been investigated as they occur again on both macroscopic (Fritz et al., 1994) and nanoscopic dimensions (Radmacher et al., 1994). Molecular interactions can now be studied with unparalleled sensitivity and resolution (Dammer et al., 1995b; Florin et al., 1994a; Lee et al., 1994b; Moy et al., 1994).

Image formation in AFM is based on forces between the tip and the sample. It was recognized early on that under certain conditions, the different contributions may be separated by suitable instruments: sample viscoelasticity by force modulation microscopy (Florin et al., 1994b) or force volume mapping (Cleveland et al., 1994), lateral forces by scanning friction microscopy (Erlandsson et al., 1988) and Coulomb forces in aqueous environments by electric double-layer imaging (Manne and Gaub, 1995), just to name a few of them. Recently, specific adhesion forces were measured with the AFM in so-called force scans (Chilkoti et al., 1995; Dammer et al., 1995; Dammer et al., 1996; Florin et al., 1994a; Lee et al., 1994; Moy et al., 1994; Hinterdorfer et al., 1996). In this paper we have expanded this approach toward mapping specific adhesion forces by affinity imaging.

Received for publication 12 April 1996 and in final form 9 October 1996.

Address reprint requests to Dr. Hermann E. Gaub, Ludwig Maximilians Universität, Lehrstuhl für Angewandte Physik, Amalienstrasse 54, 80799 München, Germany. Tel.: 49-89-2180-3173; Fax: 49-89-2180-2050; E-mail: gaub@physik.uni-muenchen.de.

0006-3495/97/01/445/04 $2.00

MATERIALS AND METHODS

Specific adhesion pattern

Biotin-avidin is a well established molecular pair that is widely used for noncovalent but long-lasting bonds between macromolecules. Several derivatives and many thermodynamic and structural data are available. The unbinding forces have been measured by several groups (Chilkoti et al., 1995; Dammer et al., 1995, 1996; Florin et al., 1994a; Lee et al., 1994a; Moy et al., 1994) and were corroborated by molecular dynamic calculations (Grubmüller et al., 1996; Schulten, personal communication). Here we have used this molecular pair to demonstrate the concept of affinity imaging with the AFM. For this purpose a pattern of streptavidin, similar to the one reported by Mazzola and Fodor (1995), was made as follows: after silanization of standard glass cover slides with epoxysilane {2% [3-(2,3-epoxypropoxy)-propyl]trimethoxysilane in 2-propanol} for 5 min, the slides were dried at 70°C for 1 h, washed with 2-propanol, and again dried at room temperature. After incubating in a dextran solution (30 wt % dextran T500 in MilliQ H_2O) for about 20 h (Löfås, 1995; Löfås and Johnson, 1990), a pattern of 200 Å-thick gold patches was deposited by evaporating through an electronmicroscope grid (2000 mesh, Plano, Marburg, Germany). Then the hydroxy groups of the dextran were converted into hydrocarboxy groups by adding bromoacetic acid (1 M bromoacetic acid in 2 M sodium hydroxide) for 16 h. *N*-hydroxysuccinimide (NHS) groups were added by incubating the samples in a solution of EDAC [1-ethyl-3-(3-dimethylamino-propyl)carbodiimide hydrochloride] and NHS (0.2 M EDAC and 0.05 M NHS) for 30 min. The lysine groups in the streptavidin (300 μg/ml streptavidin in 0.01 M sodium acetate at pH 5.0, Böhringer Mannheim, Tutzing, Germany) were allowed to bind to the NHS-activated dextran for ~12 h. Finally the glass cover slides were washed in an ethanolamine hydrochloride solution to react the active esters and to remove free streptavidin (1 M ethanolamine hydrochloride adjusted to pH 8.5 with sodium hydroxide). To avoid unspecific adhesion to the gold patches, they were blocked with bovine serum albumin (1 mg/ml in phosphate buffered saline).

The tip was functionalized in the following way: first the SiO_x layer of the standard commercially available Si_3N_4 cantilever (Digital Instruments, Santa Barbara, USA) was silanized with dimethyl-dichlor-silane. Then it was incubated in 0.1 mg biotin-bovine serum albumin (BBSA) in 1 ml phosphate buffered saline at 4°C for 24 h. The cantilever was then rinsed extensively with MilliQH_2O to remove free reagents. Unless otherwise noted all chemicals were purchased from Sigma (Deisenhofen, Germany).

Adhesion imaging

Recently several groups have suggested ways to image adhesion by modulating the imaging force and analyzing the resulting response in the deflection signal (van der Werf et al., 1994). However, because we had

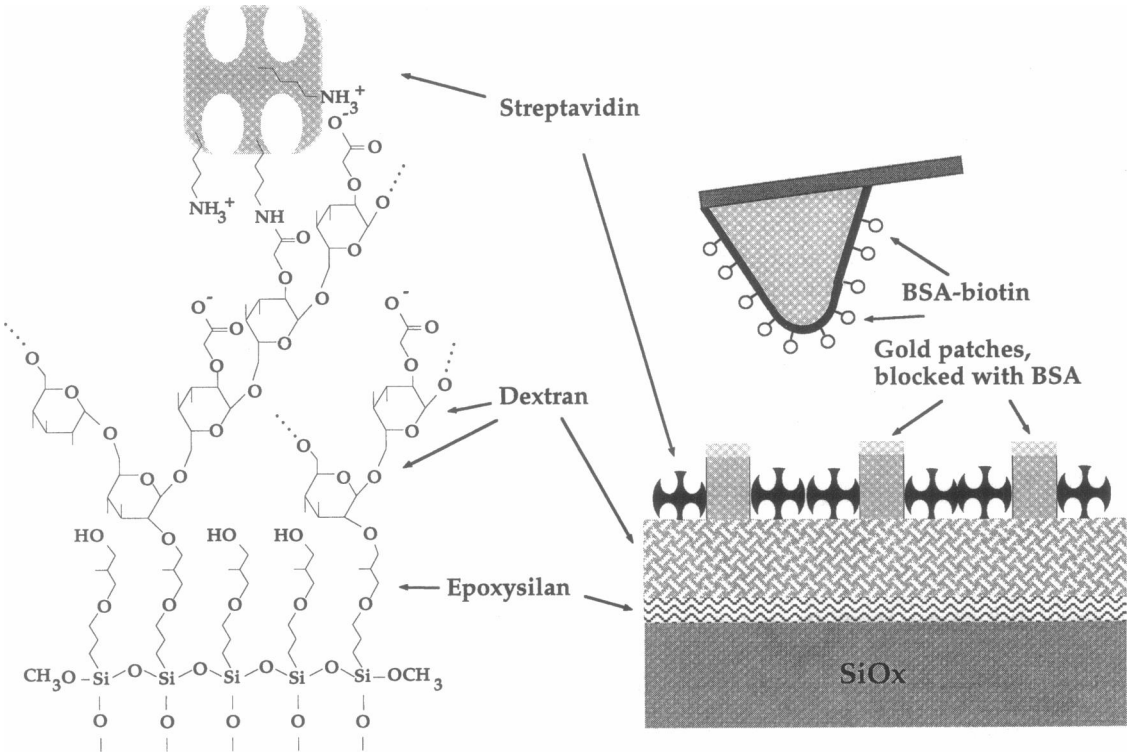

FIGURE 1 Schematics of the recognition pattern.

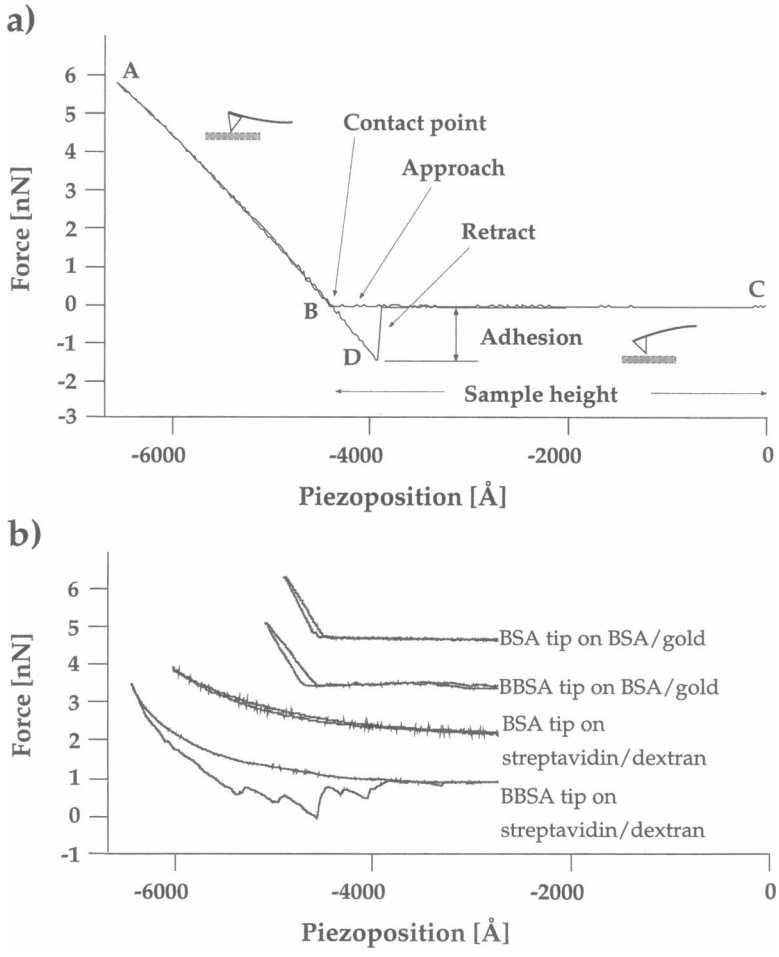

FIGURE 2 (*a*) Schematics of a force scan and the data evaluation. (*b*) Force scans recorded on different areas of the patterned sample.

learned from single molecule force measurements that nonspecific interactions may contribute significantly to the adhesion force, particularly at low forces, we felt that the recording and analysis of individual force scans would be preferable for a quantitative measurement (Fig. 1). To speed up the imaging process, we did not follow the route suggested by Cleveland et al. (1994) to first record force volumes and then to extract adhesion images offline. We developed a scheme for the online analysis of the force-distance curve taken at each point which works as follows: while lowering and raising the functionalized tip of our home-built scanned stylus-type instrument, the deflection of the cantilever, which is proportional to the force between tip and sample, is recorded. Between two force scans the data are analyzed and the sample height, the adhesion between the tip and the sample, and the elasticity of the sample are extracted. The minimum time required for a force scan was 60 ms, the maximal amplitude was 3 μm, resulting in a maximal speed of the cantilever of 5×10^{-5} m/s. The force scans were stopped and truncated in the case that the maximum indentation force between tip and sample exceeded a threshold value, in this case 5 nN. The online data analysis was performed as follows: first the approach contact (point *B*, Fig. 2 *a*) was determined by subtracting the measured approach track from the line between point *A* and point *C*. Points *C* and *A* are the start and the end point of the approach curve. Then the minimum of the difference curve was determined. The *z*-coordinate of the minimum was taken as the height signal. The elasticity of the tip-sample interaction was derived from the slope of the line *AB*, following the analysis given in Radmacher et al. (1993, 1995) and Weisenhorn et al. (1993). For the extraction of the adhesion force, the minimum of the retract trace *D* was projected onto the line *BC*, and the difference of the deflection values was used to calculate the adhesion force. In the case of faster force scans ($t < 40$ ms) the hysteresis of the piezo required a separate analysis of retract and approach curves. These three extracted values were then stored and displayed in separate gray scale windows. The spring constant of the cantilever was determined in each experiment using the thermal noise technique reported earlier (Florin et al., 1995). Values of 60 ± 5 mN/m were obtained with the cantilevers used here. The piezo was calibrated with standard calibration grids. Typical data acquisition rates in this mode are ~17 min per frame with 128 × 128 pixels. Examples for typical force scans are given in Fig. 2 *b*. The traces show the differences in elasticity between the gold-coated areas of the pattern and the uncovered dextran. The only trace that shows significant adhesion is the one between the biotin tip and the streptavidin surface. Note that in this case the unbinding occurs in several steps. Our algorithm will detect the highest step and take it as the adhesion value.

RESULTS AND DISCUSSION

In Fig. 3 the images are given that were recorded on the avidin pattern with a biotin tip. Fig. 3 *a* shows the topography image of the pattern. Clearly visible are the elevated gold squares that were evaporated onto the substrate. The height step corresponds to the deposited film thickness. In the affinity image (Fig. 3 *b*) these squares are low in affinity, whereas the areas that where covered by the meshes of the grid show high affinity. The adhesion histogram (Fig. 3 *e*) shows that the adhesion has a broad distribution and is centered at about 1000 pN. Taking into account that the unbinding force of individual molecular pairs is 250 pN, this adhesion seems to be caused by several molecular pairs in parallel. Inasmuch as the instrument used in this study is not sensitive enough to resolve the binding forces with the necessary accuracy, and the anchoring of the molecular partners had a high spring constant, we did not attempt here to discriminate among individual unbinding events.

To confirm that the measured adhesion image is due to specific molecular recognition, the sample was blocked by adding an excess of free biotin (ImmunoPure Biotin, Pierce, USA). Under these conditions virtually no contrast was measured in the affinity image (Fig. 3 *d*), whereas the topography contrast did not change (Fig. 3 *c*). To show that the tip was still functional, we tested it on streptavidin-labeled agarose beads. Here we found adhesion again, which we could block by adding free streptavidin.

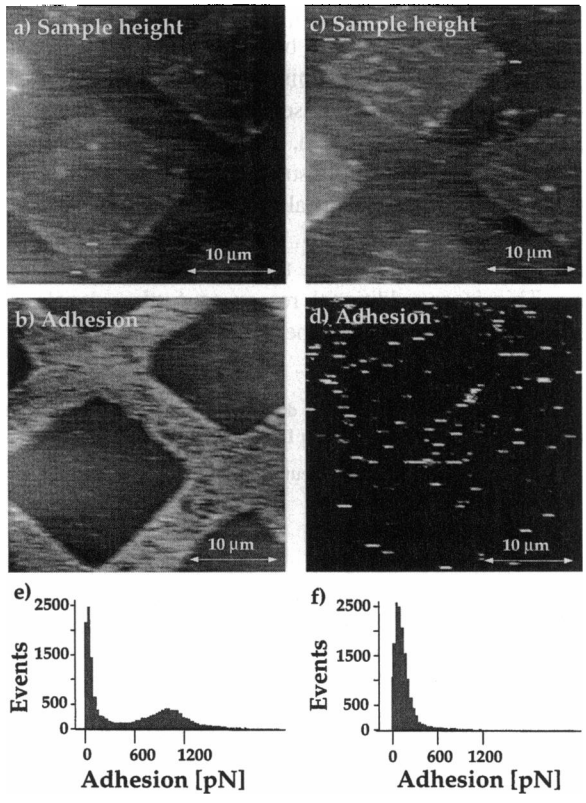

FIGURE 3 Affinity image of the streptavidin/gold pattern showing the topography images (*a* and *c*) as well as the affinity images (*b* and *d*) before and after blocking with free biotin. Adhesion histograms of images *b* and *d* are shown in *e* and *f*, respectively.

It should be noted here, however, that in many cases the tip gradually lost its sensitivity with the half-lifetime of a few images. Preliminary experiments (data not shown here) have revealed that in most cases the tip is not damaged, but rather blocked by streptavidin that was only loosely attached to the sample. A thorough and extensive washing helped in most cases to circumvent this problem.

CONCLUDING REMARKS

Affinity imaging has the potential to become a very versatile AFM imaging mode for a broad range of samples in life sciences. Here we have demonstrated that a well-defined pattern of strongly interacting molecular partners can be imaged with satisfying contrast and in a reasonable image acquisition time. An improvement in tip stability, enhanced sensitivity, and faster image acquisition are desirable to apply this technique to a wider range of "real" samples, e.g., markers on live cells. The lateral resolution is given by the

length of the spacers on the tip and the geometry of the tip. Luckily, measuring weaker binding forces is, at least in principle, easier at higher unbinding rates, so that improving this part of the experiment seems to be only an issue of technology. A basic limitation, however, is to be expected in the case of membrane-bound surface markers of cells. Several groups have shown (Evans et al., 1991; Leckband et al., 1995) that above several tens of pN, the membrane anchors of the molecules are extracted from the lipid moiety of the membrane. This is an additional reason to further develop this promising technique toward the detection of smaller forces.

We gratefully acknowledge helpful discussions with Matthias Rief, Lutz Schmitt, and technical support from Digital Instruments.

This work was supported by the Deutsche Forschungsgemeinschaft.

REFERENCES

Bezanilla, M., B. Drake, E. Nudler, M. Kashlev, P. K. Hansma, and H. G. Hansma. 1994. Motion and enzymatic degradation of DNA in the atomic force microscope. *Biophys. J.* 67:1–6.

Binnig, G., C. F. Quate, and C. Gerber. 1986. Atomic force microscope. *Phys. Rev. Lett.* 56:930.

Binnig, G., H. Rohrer, C. Gerber, and E. Weibel. 1983. 7 × 7 Reconstruction on Si(111) resolved in real space. *Phys. Rev. Lett.* 50:120–123.

Chilkoti, A., T. Boland, B. D. Ratner, and R. S. Stayton. 1995. The relation between ligand-binding thermodynamics and protein-ligand interaction forces measured by atomic force microscopy. *Biophys. J.* 69:2125–2130.

Cleveland, J. P., M. Radmacher, and P. K. Hansma. 1994. Atomic scale force mapping with the atomic force microscope. *NATO Advanced Research Workshop.* 543–549.

Dammer, U., M. Hegner, D. Anselmetti, P. Wagner, M. Dreier, W. Huber, and H.-J. Güntherodt. 1996. Specific antigen/antibody interactions measured by force microscopy. *Biophys. J.* 70:2437–2441.

Dammer, U., O. Popescu, P. Wagner, D. Anselmetti, H.-J. Güntherodt, and G. N. Misevic. 1995. Binding strength between cell adhesion proteoglycans measured by atomic force microscopy. *Science.* 267:1173–1175.

Engel, A. 1991. Biological applications of scanning probe microscopes. *Annu. Rev. Biophys. Biophys. Chem.* 20:79–108.

Erlandsson, R., G. Hadziioannou, C. M. Mate, G. M. McClelland, and S. Chiang. 1988. Atomic scale friction between the muscovite mica cleavage plane and a tungsten tip. *J. Chem. Phys.* 89:5190–5193.

Evans, E., D. Berk, and A. Leung. 1991. Detachment of agglutinin bonded red blood cells. I. Forces to rupture molecular point attachments. *Biophys. J.* 59:838–848.

Florin, E.-L., V. T. Moy, and H. E. Gaub. 1994a. Adhesion forces between individual ligand-receptor pairs. *Science.* 264:415–417.

Florin, E.-L., M. Radmacher, B. Fleck, and H. E. Gaub. 1994b. AFM with direct force modulation. *Rev. Sci. Instrum.* 65:639–643.

Florin, E. L., M. Rief, H. Lehmann, M. Ludwig, C. Dornmair, V. T. Moy, and H. E. Gaub. 1995. Sensing specific molecular interactions with the atomic force microscope. *Biosensors and Bioelectronics.* 10:895–901.

Fritz, M., M. Radmacher, and H. E. Gaub. 1994. Granula motion and membrane spreading on human platelets imaged with the AFM. *Biophys. J.* 66:1–7.

Grubmüller, H., B. Heymann, and P. Tavan. 1996. Ligand-receptor binding: molecular mechanics calculation of the streptavidin-biotin rupture force. *Science.* 271:997–999.

Hansma, H. G., and J. H. Hoh. 1994. Biomolecular imaging with the atomic force microscope. *Annu. Rev. Biophys. Biomol. Struct.* 23: 115–139.

Hansma, P. K., V. B. Elings, O. Marti, and C. E. Bracker. 1988. Scanning tunneling microscopy and atomic force microscopy: application to biology and technology. *Science.* 242:209–216.

Henderson, E., P. G. Haydon, and D. S. Sakaguchi. 1992. Actin filament dynamics in living glial cells imaged by atomic force microscopy. *Science.* 257:1944–1946.

Hinterdorfer, P., W. Baumgartner, H. J. Gruber, K. Schilcher, and H. Schindler. 1996. Detection and localization of individual antibody-antigen recognition events by atomic force microscopy. *Proc. Natl. Acad. Sci. USA.* 93:3477–3481.

Hoh, J. H., R. Lal, S. A. John, J. P. Revel, and M. F. Arnsdorf. 1991. AFM and dissection of gap junctions. *Science.* 253:1405–1408.

Leckband, D. E., W. Mueller, F.-J. Schmitt, and H. Ringsdorf. 1995. Molecular mechanisms determining the strength of receptor-mediated intermembrane adhesion. *Biophys. J.* 69:1162–1169.

Lee, G. U., L. A. Chris, and R. J. Colton. 1994. Direct measurement of the forces between complementary strands of DNA. *Science.* 266:771–773.

Löfås, S. 1995. Dextran modified self-assembled monolayer surfaces for use in biointeraction analysis with surface plasmon resonance. *Pure Appl. Chem.* 67:829–834.

Löfås, S., and B. Johnson. 1990. A novel hydrogel matrix on gold surfaces in surface plasmon resonance sensors for fast and efficient covalent immobilization of ligands. *J. Chem. Soc.* 1526–1528.

Manne, S., and H. E. Gaub. 1995. Molcular organization of surfactants at solid-liquid interfaces. *Science.* 270:1480–1482.

Mazzola, L. T., and S. P. A. Fodor. 1995. Imaging biomolecule arrays by atomic force microscopy. *Biophys. J.* 68:1653–1660.

Moy, V. T., E. L. Florin, and H. G. Gaub. 1994. Intermolecular forces and energies between ligands and receptors. *Science.* 266:257–259.

Müller, D. J., C.-A. Schoenenberger, G. Büldt, and A. Engel. 1996. Immunoatomic force microscopy of purple membrane. *Biophys. J.* 70: 1796–1802.

Radmacher, M., M. Fritz, H. G. Hansma, and P. K. Hansma. 1994. Direct observation of enzyme activity with the atomic force microscope. *Science.* 265:1577–1579.

Radmacher, M., M. Fritz, and P. K. Hansma. 1995. Measuring the elastic properties of biological materials with the atomic force microscope. *Biophys. J.* 68:A139.

Radmacher, M., R. W. Tillman, and H. E. Gaub. 1993. Imaging viscoelasticity by force modulation with the atomic force microscope. *Biophys. J.* 64:735–742.

Radmacher, M., R. W. Tillmann, M. Fritz, and H. E. Gaub. 1992. From molecules to cells—imaging soft samples with the AFM. *Science.* 257: 1900–1905.

van der Werf, K. O., C. A. J. Putman, B. G. De Grooth, and J. Greve. 1994. Adhesion force imaging in air and liquid by adhesion mode atomic force microscopy. *Appl. Phys. Lett.* 65:1195–1197.

Weisenhorn, A. L., B. Drake, C. B. Prater, S. A. C. Gould, P. K. Hansma, F. Ohnesorge, M. Egger, S. P. Heyn, and H. E. Gaub. 1990. Immobilized proteins in buffer imaged at molecular resolution by atomic force microscopy. *Biophys. J.* 58:1251–1258.

Weisenhorn, A. L., M. Khorsandi, S. Kasas, V. Gotzos, M. R. Celio, and H. J. Butt. 1993. Deformation and height anomaly of soft surfaces studied with an AFM. *Nanotechnology.* 4:106–113.

Wickramasinghe, H. K. 1990. Scanning probe microscopy: current status and future trends. *J. Vac. Sci. Technol.* A8:363–368.